

Interplay between secondary and tertiary structure formation in protein folding cooperativity

Tristan Bereau,[†] Michael Bachmann,[‡] and Markus Deserno^{*,†}

Dept. of Physics, Carnegie Mellon University, Pittsburgh, PA 15213, USA, and Institut für Festkörperforschung, Theorie II, Forschungszentrum Jülich, 52425, Jülich, Germany

Received February 7, 2022; E-mail: deserno@andrew.cmu.edu

The folding cooperativity of proteins is characterized by the relative population of intermediate states at the transition temperature: while two-state transitions exhibit two energetic peaks characterizing the folded and unfolded ensembles, downhill folders show a unimodal distribution of energetic states without any barrier.^{1,2} This aspect of finite-size thermodynamic transitions can provide insight into the folding mechanism, but energetic populations can be difficult to measure. Therefore, protein folding cooperativity is often probed using the calorimetric criterion,³ which quantifies the sharpness of the specific heat curve. From a computer simulation point of view, however, evaluating the probability density $p(E)$ remains an appealing idea, as it would provide an unambiguous description of the thermodynamic transition. Although currently untractable atomistically due to sampling limitations, high resolution coarse-grained models offer an alternative approach.⁴ While cutting down significantly on computational time, they can retain much chemical detail, and some are even able to fold simple peptides with no prior knowledge of the native state. In this Communication we study the link between thermodynamics and structure for helical peptides using such a coarse-grained model,⁵ details of which can be found in the Supporting Information.

To characterize the thermodynamics of finite-size systems, it has been shown that a microcanonical analysis, based on the entropy $S(E)$, is often more informative than a canonical analysis.^{6,7} Microcanonically, $S(E) = k_B \ln \Omega(E)$ where $\Omega(E)$ is the density of states. One remarkable feature of such a description is its ability to unambiguously distinguish between discontinuous (*i. e.*, two-state) and continuous (*i. e.*, downhill) transitions. Indeed, two-state transitions exhibit a depletion of intermediate energetic states leading to local convexity in the entropy. This can be best observed by defining the quantity $\Delta S(E) = \mathcal{H}(E) - S(E)$, where the first term is the (double-)tangent to $S(E)$ in the transition region.^{8–10} The method relies on accurate measurements of the density of states, calculated here using the Weighted Histogram Analysis Method.¹¹ All order parameters will be analyzed as a function of energy.

We first examine a short α -helix of sequence (AAQAA)₃.¹² The density of states reveals a discontinuous transition with nonzero latent heat ΔQ ([figure][1][1], a) between the folded and unfolded ensembles (representative conformations at different energies are shown). Phase coexistence is associated with a backbending⁶ of the microcanonical inverse temperature $T_{\mu c}^{-1} = \partial S / \partial E$ while the corresponding canonical relation $T^{-1}(\langle E \rangle_{\text{can}})$, where $\langle E \rangle_{\text{can}}$ is the average energy, is monotonic ([figure][1][1], b). The radius of gyration ([figure][1][1], c) quickly drops inside the coexistence region, indicating that most structural rearrangements happen within this energy interval. We will assume the hydrogen-bond and side chain energies, E_{hb} and E_{sc} , to be suitable proxies of secondary structure and tertiary contacts, respectively. It proves instructive to look at their energetic rates, dE_{hb}/dE and dE_{sc}/dE ([figure][1][1], d):

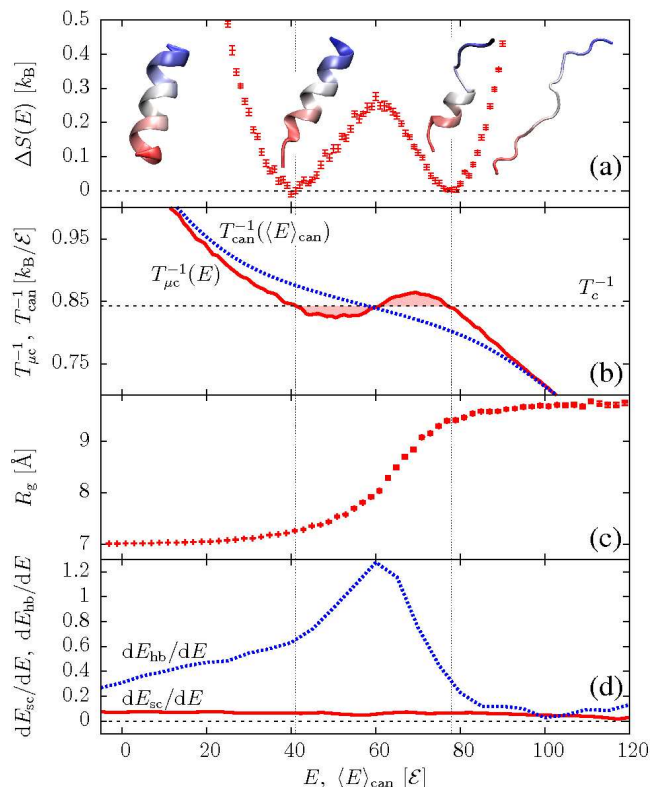


Figure 1. (AAQAA)₃. (a) $\Delta S(E)$; error bars reflect the variance of the data points (1σ interval). (b) inverse temperature from a canonical $T_{\text{can}}^{-1}(\langle E \rangle_{\text{can}})$ and microcanonical $T_{\mu c}^{-1}(E) = \partial S / \partial E$ analysis, where $\langle E \rangle_{\text{can}}$ is the canonical average energy. (c) radius of gyration $R_g(E)$ with the error of the mean. (d) rates of H-bond and side chain energies dE_{hb}/dE , dE_{sc}/dE . Vertical lines delimit the transition region; its width corresponds to the microcanonical latent heat ΔQ .

even though dE_{sc}/dE stays virtually flat over the energy range considered, the sharp peak in dE_{hb}/dE indicates that most secondary structure forms within the coexistence region.

Elongating the sequence to (AAQAA)₁₅ leads to a qualitative change in the folding mechanism. The ground state again forms a single α -helix, but the transition is now continuous: as can be seen in [figure][2][1] (a) and Figure S2 (Supporting Information), there is a single transition point and the latent heat is zero. The radius of gyration ([figure][2][1], b) features a sharp minimum *above* the transition point, indicative of a chain collapse into “maximally compact non-native states.”¹³ Upon lowering the energy further, the chain will reorganize from such non-native states into the helical state. In doing so, the rate of tertiary contact formation dE_{sc}/dE dips below zero ([figure][2][1], c), hence there is an energetic penalty associated with tertiary rearrangements. Hydrogen-bond formation occurs over a large energetic interval as indicated by the broad maximum in dE_{hb}/dE . The absence of any two-state signal

[†]Carnegie Mellon University

[‡]Forschungszentrum Jülich

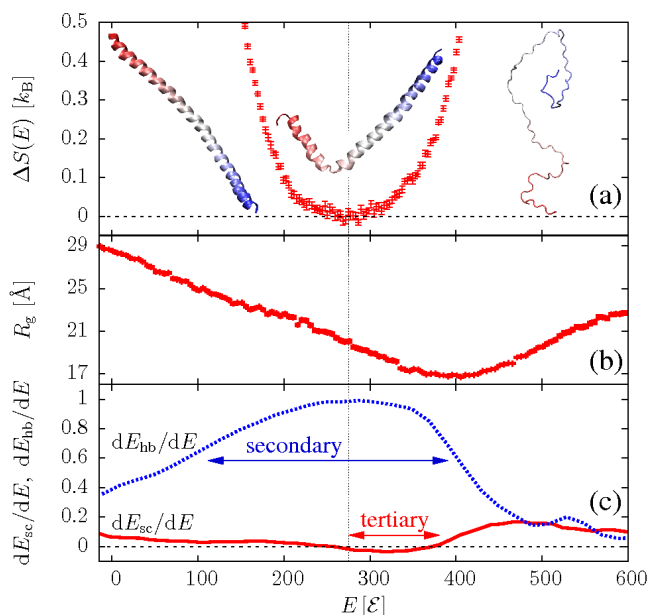


Figure 2. (AAQAA)₁₅. (a) $\Delta S(E)$. (b) radius of gyration $R_g(E)$. (c) rates of H-bond and side chain energies dE_{hb}/dE , dE_{sc}/dE . Horizontal arrows indicate where most secondary structure forms and where non-native tertiary contacts dissolve. The vertical line marks the transition point.

is consistent with theoretical models of the helix-coil transition:¹⁴ the energetic cost of breaking a hydrogen-bond is outweighed by the conformational entropy gained. Further analysis indicates on average two helices at the transition point.

While of similar length, the 73 amino acid *de novo* three-helix bundle $\alpha 3D$ (PDB code: 2A3D)¹⁵ does show a discontinuous transition, see [figure][3][3] (a). Representative conformations sampled in the two coexisting ensembles stand as good proxies of the ground state and unfolded state, unlike for the downhill folding transition of (AAQAA)₁₅. The radius of gyration again shows a minimum above the transition ([figure][3][3] (b)), and folding once more starts from maximally compact non-native states. Notice that secondary structure formation and the loss of non-native tertiary contacts ([figure][3][3] (c)) are sharp and predominantly localized within the coexistence region. The three helices form inside the same energetic interval due to the inter-helical cooperativity imprinted in the sequence.¹⁶ Chain compaction is due to strong side chain-side chain interactions.

Overall, we can correlate thermodynamic features with structural information from the three peptides studied here. While (AAQAA)₃ is too short for tertiary interactions to play any role, the transitions associated with (AAQAA)₁₅ and the bundle $\alpha 3D$ are both associated with tertiary rearrangements. These two examples suggest that independently of its nature, the folding transition is driven by the loss of non-native tertiary contacts (*i. e.*, the region where $dE_{sc}/dE < 0$)—reminiscent of the heteropolymer collapse model.¹³ On the other hand, secondary structure formation has shown very different signals: (AAQAA)₃ and $\alpha 3D$ exhibit sharp peaks where (AAQAA)₁₅ displays a broad maximum. As shown in [figure][2][2] (c), secondary structure formation in a downhill folding peptide occurs over a much broader interval compared to the loss of non-native tertiary contacts, whereas these two quantities are contained within the same narrow interval for a two-state peptide ([figure][3][3] (c)). Cooperative secondary and tertiary structure formation has been proposed as a mechanism for two-state folding from lattice simulations¹⁷ and theoretical models.¹⁶ Beyond this, our results also highlight the interplay between secondary structure formation and the loss of non-native tertiary contacts. Our conclu-

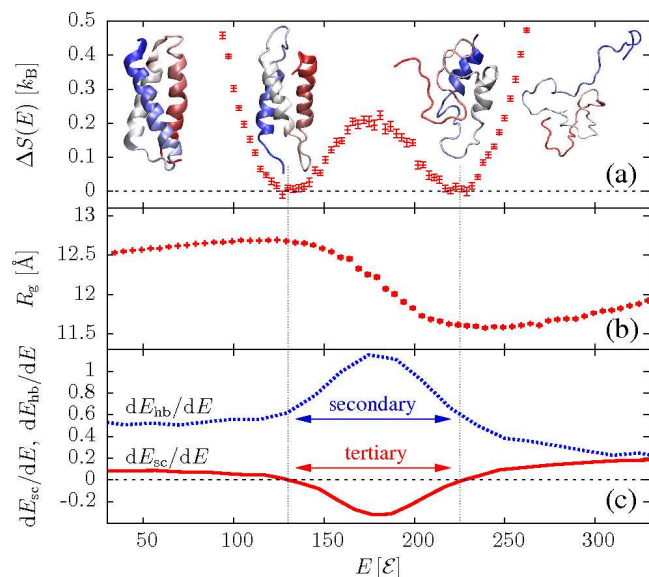


Figure 3. Three-helix bundle $\alpha 3D$. (a) $\Delta S(E)$. (b) radius of gyration $R_g(E)$. (c) rates of H-bond and side chain energies dE_{hb}/dE , dE_{sc}/dE .

sions on the thermodynamics of the short-, long-, and bundled helix are compatible with the calorimetric criterion, which gives, respectively, $\delta = 0.78$, 0.52 , 0.78 for the calorimetric ratio.³ Note that Ghosh and Dill¹⁶ predicted $\delta = 0.72$ for the similar bundle $\alpha 3C$. However, the main strength of a microcanonical analysis stems from an access to fine aspects of thermodynamic information that are otherwise difficult to obtain either canonically or from experiments. It thus stands as a complementary tool to gain further insight.

Acknowledgement

We acknowledge stimulating discussions with K. Binder, W. Paul, R.H. Swendsen, and M. Taylor, and funding through the NIH grant P01AG03231. MB thanks the Forschungszentrum Jülich for supercomputer time grants jiff39 and jiff43. TB acknowledges support from the Astrid and Bruce McWilliams Fellowship.

Supporting Information Available

Peptide model; simulation and analysis methods.

References

- (1) Privalov, P. *Adv. Prot. Chem.* **1979**, *33*, 167–241
- (2) Privalov, P. *Adv. Prot. Chem.* **1982**, *35*, 1–104
- (3) Kaya, H.; Chan, H. *Proteins* **2000**, *40*, 637–661
- (4) Voith, G. *Coarse-Graining of Condensed Phase and Biomolecular Systems*; Taylor & Francis, New York, 2008
- (5) Bereau, T.; Deserno, M. *J. Chem. Phys.* **2009**, *130*, 235106
- (6) Gross, D. *Microcanonical Thermodynamics: Phase Transitions in 'Small' Systems*; World Scientific Publishing Company, 2001
- (7) Hüller, A. *Zeitschrift für Physik B* **1994**, *93*, 401–405
- (8) Deserno, M. *Phys. Rev. E* **1997**, *56*, 5204
- (9) Junghans, C.; Bachmann, M.; Janke, W. *Phys. Rev. Lett.* **2006**, *97*, 218103
- (10) Junghans, C.; Bachmann, M.; Janke, W. *J. Chem. Phys.* **2008**, *128*, 085103
- (11) Kumar, S.; Rosenberg, J.; Bouzida, D.; Swendsen, R.; Kollman, P. *J. Comput. Chem.* **1995**, *16*, 1339–1350
- (12) Scholtz, J.; York, E.; Stewart, J.; Baldwin, R. *J. Am. Chem. Soc.* **1991**, *113*, 5102–5104
- (13) Dill, K.; Stigter, D. *Adv. Protein Chem.* **1995**, *46*, 59–104
- (14) Zimm, B.; Bragg, J. *J. Chem. Phys.* **1959**, *31*, 526
- (15) Walsh, S.; Cheng, H.; Bryson, J.; Roder, H.; Degrad, W. *Proc. Natl. Acad. Sci.* **1999**, *96*, 5486–5491
- (16) Ghosh, K.; Dill, K. *J. Am. Chem. Soc.* **2009**, *131*, 2306–2312
- (17) Kaya, H.; Chan, H. *Phys. Rev. Lett.* **2000**, *85*, 4823–4826

Abstract

Protein folding cooperativity is defined by the nature of the finite-size thermodynamic transition exhibited upon folding: two-state transitions show a free energy barrier between the folded and unfolded ensembles, while downhill folding is barrierless. A microcanonical analysis, where the energy is the natural variable, has shown better suited to unambiguously characterize the nature of the transition compared to its canonical counterpart. Replica exchange molecular dynamics simulations of a high resolution coarse-grained model allow for the accurate evaluation of the density of states, in order to extract precise thermodynamic information, and measure its impact on structural features. The method is applied to three helical peptides: a short helix shows sharp features of a two-state folder, while a longer helix and a three-helix bundle exhibit downhill and two-state transitions, respectively. Extending the results of lattice simulations and theoretical models, we find that it is the interplay between secondary structure and the loss of non-native tertiary contacts which determines the nature of the transition.